

First-Principles Calculations of the Electronic Properties of Silicon Quantum Wires

A. J. Read,⁽¹⁾ R. J. Needs,⁽¹⁾ K. J. Nash,⁽²⁾ L. T. Canham,⁽²⁾ P. D. J. Calcott,⁽²⁾ and A. Qteish⁽¹⁾

⁽¹⁾*Cavendish Laboratory, University of Cambridge, Cambridge CB3 0HE, United Kingdom*

⁽²⁾*Defence Research Agency Malvern (Royal Signals and Radar Establishment), Malvern, Worcester WR14 3PS, United Kingdom*

(Received 18 May 1992)

We have performed first-principles pseudopotential calculations for H-terminated Si wires with thicknesses from 12 to 23 Å, calculating the band gaps and optical matrix elements. Comparison with effective-mass theory shows that the latter is valid for wires wider than 23 Å. We have used our data to analyze the luminescent properties of highly porous Si fabricated by electrochemical etching of Si wafers in HF-based solutions.

PACS numbers: 71.25.-s, 73.20.Dx, 85.60.Jb

A great deal of interest has been stimulated by the demonstration that a simple electrochemical etching process can create crystalline Si nanostructures which show efficient visible luminescence at room temperature [1]. This contrasts with the behavior of bulk crystalline Si, whose indirect band gap at room temperature of 1.11 eV results in near-infrared luminescence of very low efficiency. There is a vigorous debate concerning the origin of these dramatic differences in emission wavelength and efficiency. The development of Si-based optical sources has long been a goal of semiconductor research, since such devices would find widespread application, for example, as optical interconnects in very-large-scale integration (VLSI) systems and as high-resolution displays.

Electrochemical etching of bulk Si wafers in HF-based solutions can generate porous structures whose crystalline Si skeleton has remarkably small dimensions. Indeed recent transmission electron microscopy (TEM) studies [1] have demonstrated that under suitable conditions this etching process can generate isolated columns of width < 50 Å. With such small sizes substantial quantum size effects are expected [2], which Canham [3] has suggested can account for the shorter photoluminescence (PL) wavelength of porous Si compared with bulk Si. The assignment of the visible PL of porous Si to quantum-confined carriers in crystalline Si is still controversial. An alternative suggestion, for example, is that the PL is due to siloxene [4], a Si-based polymer. Other groups agree with the quantum-confinement model, but suggest zero-dimensional structures (dots) [5], rather than the essentially one-dimensional wires favored by Canham [3].

In this work we calculate the optical properties of perfect H-terminated Si wires using a first-principles technique. We calculate the band gaps and compare them with observed quantum upshifts. The calculated optical matrix elements are used to estimate the radiative lifetime of localized exciton states in a narrow Si wire, which is compared with experiment. We model the isolated columns of porous Si as wires of rectangular cross section with the wire axis along the [001] direction, and wire surfaces which correspond to (110) surfaces of bulk Si. Each surface dangling bond is saturated by a H atom, reflecting the hydride passivation of HF-treated Si sur-

faces [3,6]. The structure of the narrowest wire considered is illustrated in Fig. 1. This wire has twenty Si atoms per unit cell which, when viewed along the wire axis, form a rectangular array. We refer to this as a "5×4 wire." It is simple to make analogous structures of (N+1)×N form and we have also studied 7×6 and 9×8 wires, in order to obtain trends in properties with wire thickness. The thickest of these wires, the 9×8 structure, is comparable in width to the thinnest of the wires observed in TEM studies of porous Si [1]. We take the Si-H bond length to be 1.637 Å, which was obtained from a cluster calculation [7], and use the experimental value for the bulk Si-Si separation of 2.351 Å. We use a supercell method in which the basic unit cell is repeated throughout space to retrieve three-dimensional periodicity. For each wire thickness we make a rectangular array of wires with the shortest distance between H atoms on adjacent wires being 5 Å, and the interactions between adjacent wires were found to be negligible. In addition the effects of relaxation of the atomic positions of the 5×4 wire were studied and found to be very small.

For our calculations we employed a first-principles pseudopotential technique, using the norm-conserving pseudopotential for the Si⁴⁺ ions from Ref. [8] and the bare Coulomb potential for the H⁺ ions. We used the Wigner form [9] of the local-density approximation (LDA) for the exchange-correlation energy and potential.

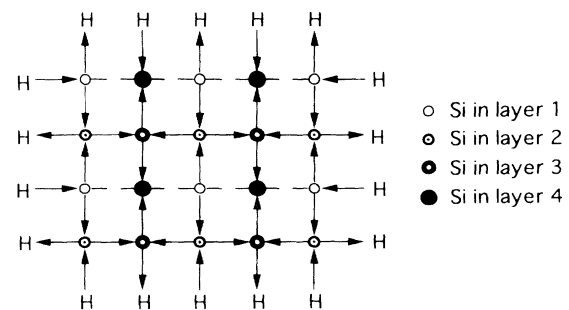


FIG. 1. Cross-sectional view of the 5×4 wire structure. The hydrogen atoms are denoted by H. The directions of the arrows indicate bonds which project out of the plane of the paper.

Brillouin zone integrations were performed by sampling on a regular $2 \times 2 \times 2$ grid of points in reciprocal space, except for bulk Si where a $4 \times 4 \times 4$ grid was used. All results reported in this paper were obtained using a plane-wave basis set containing waves up to a cutoff energy of 6 Ry. Tests on bulk Si and on the 5×4 wire using larger cutoffs show that using this truncated basis set places the low-lying conduction-band states, when measured with respect to the valence-band maximum, between 0.3 and 0.5 eV higher in energy than a fully converged calculation. The relatively small basis set cutoff of 6 Ry does not provide an accurate description of electronic states with a large weight on the H atoms, but such states are situated well away from the band-gap region and are not of interest in this study. The effective masses of bulk Si relevant to the quantum-confinement problem within effective-mass theory (EMT) (see below) are given to within 10% in our calculations. The difference between our calculated band gap of 0.78 eV and the experimental low-temperature value of 1.17 eV [10] is due to our use of the local-density approximation and the truncation of the basis set. However, the confinement effects that we are interested in should be well accounted for in our calculations and the one-electron wave functions should yield realistic values for optical matrix elements.

The band structure of the wires is one dimensional, and the fundamental band gap is expected to be direct and at the zone center. This result can be obtained from the following EMT argument, which applies for thick wires. In bulk Si the band gap is indirect, with the valence-band maximum at the zone center. There are six equivalent conduction-band minima at $\pm(0,0,0.85)2\pi/a_0$, $\pm(0,0.85,0)2\pi/a_0$, and $\pm(0.85,0,0)2\pi/a_0$, where $a_0 = 5.429$ Å is the lattice constant of bulk Si. These minima are ellipsoidal with a transverse mass of $m_T = 0.1905$ and a longitudinal mass of $m_L = 0.9163$ [10]. On formation of a [001]-oriented wire the conduction-band minima at $\pm(0,0,0.85)2\pi/a_0$ are upshifted in energy by a large amount, because of their small mass (m_T) in the confinement plane. The other four conduction-band minima are also upshifted, but by a smaller amount because they have one transverse and one longitudinal mass in the confinement plane. Hence the conduction-band edge of a [001]-oriented wire is expected to be derived from the $\pm(0,0.85,0)2\pi/a_0$ and $\pm(0.85,0,0)2\pi/a_0$ states of bulk Si and thus comprises four minima very close in energy. These states are folded onto the zone center of the wire band structure to form the conduction-band minimum. The valence-band maximum of Si is at the zone center and therefore the band gaps of the wires are expected to be direct and at the zone center.

To aid comparison with experimental data we quote our results as a function of the wire thickness d defined by

$$d = a_0 \sqrt{M} / 2, \quad (1)$$

where M is the number of Si atoms per unit cell, i.e., M is

20, 42, and 72 for the 5×4 , 7×6 , and 9×8 wires, respectively. For each wire structure the Si-H bonding is strong enough to remove from the band-gap region the states which have a large weight on the H atoms, and so these states play only a very small role in the valence-band maximum and conduction-band minimum states. For each wire structure the band gap was found to be direct and at the zone center. In Fig. 2 we show our results for the upshift of the lowest band gaps of the wire structures. The band gap increases as the wire thickness decreases because of the confinement effect. We have also calculated the band structure of a polysilane molecule, which represents the narrowest wire achievable, obtaining a direct band gap at the zone center of 4.69 eV. Taking the data shown in Fig. 2 together with the polysilane result gives the trend in the energy gap across the entire range of wire thicknesses from bulk Si to polysilane. For the 9×8 wire the four lowest conduction-band states have an energy range of 25 meV, and are separated from the next conduction-band state by 160 meV. This is in accordance with the EMT picture presented above. For the thinner 7×6 and 5×4 wires, the four lowest conduction-band states are spread over 70 and 161 meV, respectively; however, these states are only 90 meV below the next conduction-band state for the 7×6 wire, and 86 meV for the 5×4 wire, so that there is no real separation between the lowest four states and the next state.

We now compare the calculated band gaps with the results of EMT. We assume that the wire has a square cross section of side d and (110)-type surfaces. For the valence-band maximum we neglect the spin-orbit splitting as in our first-principles calculations and treat the three-fold degenerate band edge exactly. The EMT band-gap upshift is then given by

$$\Delta = \left[2(\gamma_1 - 2\gamma_2) + \left(\frac{1}{m_T} + \frac{1}{m_L} \right) C \left(\frac{m_T}{m_L} \right) \right] \frac{\hbar^2 \pi^2}{2d^2}, \quad (2)$$

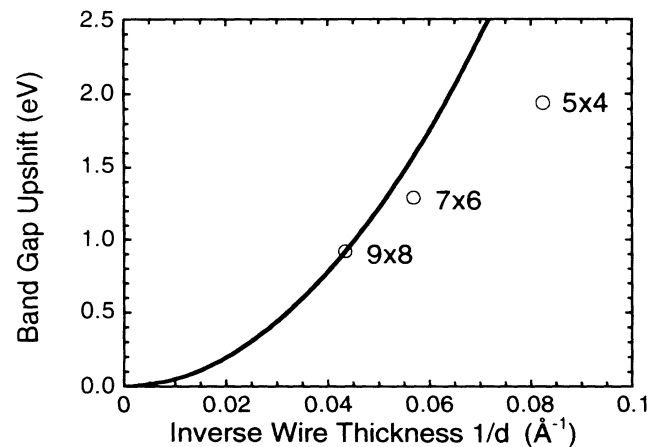


FIG. 2. The band-gap upshift of the wire structures with respect to bulk Si plotted against the inverse of the wire thickness (circles). The EMT upshift of Eq. (2) with $C=0.900$ is also plotted (continuous line). The wire thickness d is defined by Eq. (1).

where $\gamma_1=4.285$ and $\gamma_2=0.339$ are valence-band Luttinger parameters [10]. The function $C(m_T/m_L)$ cannot be obtained analytically; however, the simplest particle-in-a-box approximation gives $C=1$ and a full numerical solution using the Si masses gives $C=0.900$ [11]. The EMT curve with $C=0.900$ is plotted in Fig. 2 and passes very close to the result of the full calculation for the 9×8 wire. For the 9×8 wire the EMT results and the full calculations agree in both the magnitude of the upshift and the form of the lowest conduction bands. We conclude that the EMT gives a good description of the electronic states for the 9×8 wire and thus for wires wider than 23 Å, but thinner wires show significant deviations from the EMT picture.

We now compare our calculated results with experiment, concentrating on material with $\sim 80\%$ porosity formed by anodization of lightly doped p -type Si wafers in ethanoic HF. Such material has been well characterized [1,11] and exhibits efficient PL. In particular we consider the p -type sample (No. 4) of Ref. [1]. For this sample, the average wire width found by TEM is ~ 30 Å. The nature of the luminescent states can be inferred from TEM images, which indicate that the wire thickness undulates on a length scale of ~ 40 Å. These fluctuations will cause variations in the quantum upshift along the wire, and hence a random effective potential for the motion of carriers along the wire. The amplitude of the thickness variations is approximately ± 10 Å, corresponding to potential fluctuations of several tenths of a volt. This result suggests very strongly that the carriers are localized, and separated from the delocalized states by a large activation energy. This picture is consistent with the extremely high electrical resistivity of highly porous Si [12]. Furthermore the exciton binding energy is much larger than the bulk Si value of 14.3 meV, both because of quantum confinement [13] and because the effective dielectric constant of a wire surrounded by air is smaller than that of bulk Si [14]. Therefore it is very likely that the PL, even at room temperature, is due to localized excitons, and we make this assumption in our calculations of radiative lifetimes. The measured refractive index is isotropic [11], indicating that the wires are randomly oriented. The peak photon energy of room temperature PL, $\hbar\omega_L$, is 1.48 eV, the PL appearing red to the naked eye. The PL energy should be smaller than the band-gap energy because of the binding and localization energies of the luminescent exciton, whose sum we call E_B . For a wire of the type modeled by Eq. (2), and with cross-sectional area equal to that of a 30-Å-diam cylinder, the EMT of Eq. (2) with $C=0.900$ predicts a band gap of 1.80 eV. Thus our calculations show that the experimental PL energy and wire width are consistent with the explanation that the energy gap is upshifted by quantum confinement. Our results show that E_B is large, of order 0.32 eV.

The measured value of the PL lifetime is 46 μs [11] at the peak PL energy $\hbar\omega_L=1.74$ eV for an "aged" sample

[15]. Purely radiative lifetimes τ are generally longer than measured lifetimes because the latter have contributions from nonradiative processes. We have assessed the contribution from nonradiative processes by a separate experiment on a sample immersed in HF. This treatment is known to suppress nonradiative processes by passivating the surface [6], and gives a measured lifetime of 65 μs . This indicates that the radiative lifetime is 65 μs and that nonradiative processes do not make a large contribution to the lifetime (46 μs) of aged material measured in air.

To enable us to estimate radiative lifetimes we have calculated the zone-center interband optical matrix elements for our wire structures. The radiative lifetime of a localized exciton in a direct-gap semiconductor is given by [16]

$$\frac{1}{\tau} = \frac{2\alpha\omega n}{3m^2c^2} |\langle v, k=0 | p_z | c, k=0 \rangle|^2 I,$$

where α is the fine-structure constant, ω is the photon angular frequency, n is the refractive index, m is the free-electron mass, c is the velocity of light, and p_z is the component of the momentum operator along the wire axis. The matrix element is calculated between the band-edge Bloch orbitals of the wire (the corresponding matrix element in bulk Si vanishes because of momentum conservation). For this purpose we neglect the energy splitting between the singlet and triplet exciton states and assume their populations to be in the ratio 1:3. The excitonic factor is $I = |\int dx \Phi(x, x)|^2$, where $\Phi(x_e, x_h)$ is the envelope function of the exciton. I enhances the oscillator strength for loosely bound or free excitons, and increases the free-exciton oscillator strength in systems of reduced dimensionality. In the present case we assume that the exciton is localized on a length scale comparable to the quasi-one-dimensional effective Bohr radius of the free exciton, so that $I \approx 1$ (i.e., there is no excitonic enhancement). We neglect the matrix elements of p_x and p_y (which are small compared with that of p_z) and whose contribution to $1/\tau$ is further reduced by the depolarization effect for electric fields perpendicular to the wire axis. To estimate the squared matrix element for the lowest-energy transition of a wire of unknown cross-sectional shape, we average the values calculated using our first-principles technique for the four lowest-lying conduction bands of our 9×8 structure. Using the experimental value $n=1.2$ [11] and approximating the photon energy as the band-gap energy we find $\tau=380$ μs . This is inevitably a crude estimate because without detailed information on the localizing potential for the exciton there must be uncertainty about both the size of I and the contribution to τ from higher energy bands of the wire. The localized-exciton wave function will have admixtures of these higher energy bands due to mixing by the electron-hole interaction and by disorder. With these considerations in mind, our estimate of τ is in acceptable agreement with the measured radiative lifetime of 65 μs [11].

The external radiative efficiency of highly porous Si can be orders of magnitude higher than that of bulk Si. The radiative processes occur without phonon participation because the momentum selection rule is broken by quantum confinement. A radiative lifetime longer than 380 μs is expected for wires wider than our 9×8 structure. The calculated radiative lifetime is much longer than the radiative lifetime of 1 ns for bound excitons in the direct-gap semiconductor GaAs [17], suggesting that the lifting of the momentum selection rule is not the main reason for the high radiative efficiency of porous Si. Several other factors contribute significantly to the high radiative efficiency of porous Si. Quantum confinement increases the exciton binding and localization energies, so that the luminescence arises from fast excitonic processes rather than slow band-to-band recombination. The external radiative efficiency [18] is significantly enhanced by the low refractive index [11] (compared with the bulk value), which is a consequence of the high porosity of the structure. Most remarkable is the low rate of nonradiative recombination. The hydride passivation of the surface reduces the number of surface recombination centers per unit area [3,6]. The small cross section of the wires means that the number of nonradiative centers per unit length of wire is very small, whether these centers are distributed over the surface or throughout the bulk [19]. Migration to these nonradiative defects is suppressed by exciton localization [1].

In conclusion, our first-principles study of the optical properties of Si wires gives an understanding of the energy gap across the entire range of wire thicknesses from bulk Si to polysilane. The band gaps of the wire structures were calculated to be direct and at the zone center. Because of quantum confinement the band gap increases as the wire thickness decreases. Our first-principles results are in excellent agreement with the effective-mass-theory (EMT) results for the thickest of the wires that we have studied (23 \AA), but substantial deviations from EMT occur for thinner wires. Our results, together with TEM data on the thickness of luminescent structures, show that the larger luminescence energy in porous Si compared with bulk Si is consistent with quantum confinement. Although the breakdown of the momentum selection rule enhances the interband optical matrix elements (to values consistent with experiment), it is not the main reason for the radiative efficiency of structures that emit orange or longer-wavelength light. Several factors contribute to the high efficiency, notably the enhancement of the exciton binding and localization energies by

quantum confinement, and the low rate of nonradiative recombination.

A.J.R. and A.Q. thank DRA Malvern for financial support. We thank M. I. J. Beale, A. G. Cullis, M. J. Kane, M. S. Skolnick, and D. R. Wight for critical comments on the manuscript.

-
- [1] A. G. Cullis and L. T. Canham, *Nature (London)* **353**, 335 (1991).
 - [2] V. Lehmann and U. Gösele, *Appl. Phys. Lett.* **58**, 856 (1991).
 - [3] L. T. Canham, *Appl. Phys. Lett.* **57**, 1046 (1990).
 - [4] M. S. Brandt *et al.*, *Solid State Commun.* **81**, 307 (1992).
 - [5] Y. H. Xie *et al.*, *J. Appl. Phys.* **71**, 2403 (1992).
 - [6] E. Yablonovitch *et al.*, *Phys. Rev. Lett.* **57**, 249 (1986).
 - [7] R. Jones, *J. Phys. C* **20**, L271 (1987).
 - [8] G. Bachelet *et al.*, *Phys. Rev. B* **24**, 4745 (1981).
 - [9] E. P. Wigner, *Phys. Rev.* **46**, 1002 (1934).
 - [10] *Physics of Group IV Elements and III-V Compounds, Landolt-Börnstein New Series*, edited by O. Madelung (Springer, New York, 1982), Vol. 17a, and references therein.
 - [11] P. D. J. Calcott and K. J. Nash (unpublished).
 - [12] $> 10^{11} \Omega \text{ cm}$ measured by N. Koshida, Y. Kiuchi, and S. Yoshimura (to be published).
 - [13] G. Bastard *et al.*, *Phys. Rev. B* **26**, 1974 (1982); T. Ogawa and T. Takagahara, *Phys. Rev. B* **44**, 8138 (1991).
 - [14] L. V. Keldysh, *Pis'ma Zh. Eksp. Teor. Fiz.* **29**, 716 (1979) [*JETP Lett.* **29**, 658 (1979)]; M. Kumagai and T. Takagahara, *Phys. Rev. B* **40**, 12359 (1989).
 - [15] This sample is identical to the one discussed earlier, except that it is two years old. Atmospheric impregnation leads to a more photostable structure and to an increased quantum upshift [L. T. Canham *et al.*, *J. Appl. Phys.* **70**, 422 (1991)], the PL appearing orange to the naked eye. Assuming E_B to be independent of wire width, the value of $\hbar\omega_L$ is the same as for a nonoxidized sample with columns 23 \AA wide, which corresponds to the 9×8 structure of the present work.
 - [16] Using the method of C. H. Henry and K. Nassau, *Phys. Rev. B* **1**, 1628 (1970).
 - [17] C. J. Hwang, *Phys. Rev. B* **8**, 646 (1973).
 - [18] T. S. Moss, *Optical Properties of Semiconductors* (Butterworths, London, 1959), p. 100.
 - [19] A bulk defect density of 10^{15} cm^{-3} and a surface density of $2.5\times 10^7 \text{ cm}^{-2}$ (the latter estimated for an etched Si surface in HF [6]) correspond to linear densities in a 30- \AA -wide cylindrical wire of 70 and 20 cm^{-1} , respectively.